Robust vertical takeoff and landing aircraft control via integral sliding mode

Y.J. Huang, T.C. Kuo and H.K. Way

Abstract: Reduced equivalent systems have inherent closed-loop poles at the origin in the sliding mode for conventional sliding mode control (SMC). A systematic design strategy is developed for arbitrarily placing all SMC closed-loop poles. The speed control of a vertical takeoff and landing aircraft whose aerodynamic parameters vary considerably during flight is investigated. An outstanding output tracking performance and robustness against system parameter uncertainties and external disturbances are achieved.

1 Introduction

Sliding mode control (SMC), developed from the variable structure system theory, is a powerful technique because of its capability for attaining a low sensitivity to plant parameter variations and external disturbance rejection [1, 2].

With a suitable control law the system trajectory is driven to a switching surface and remains on it thereafter. The control system is then known to be in the sliding mode. During sliding motion, the state motion is constrained to lie on the intersection of a q-dimensional sliding hypersurface. The order of the controlled system is reduced because the n-dimensional state trajectory is governed by n-q states, i.e. there are q closed-loop poles inherently at the origin [3].

Many methods have been proposed for sliding hypersurface design so that the closed-loop poles can be placed. These methods include the optimal control approach [4], geometric approach [5, 6], and algebraic approach [7]. However, the results from these methods are incomplete and only the n-q poles could be assigned. The entire control system performance cannot be freely specified with the proposed pole assignment algorithms.

We now present an improved SMC design strategy to overcome the inherent disadvantage of conventional SMC design. All the closed-loop poles can be arbitrarily placed, not just those for the reduced system in the sliding mode as in the prevailing literature. A complete design procedure including the sliding function definition, the control law formulation, and the stability proof for the feedback system are given. The sliding function involves the integral of output errors as well as the state. The control law consists of a nominal continuous part and a switching part. The resulting control system has the following advantages. All of the closed-loop poles can be assigned. The output errors converge to zero effectively and robust closed-loop system performance is achieved.

A vertical takeoff and landing (VTOL) aircraft speed control system [8, 9] design is carried out. Although the external disturbances take place due to environmental changes and the plant parameters vary with different operating conditions, the proposed SMC control system is asymptotically stable and the output errors converge to zero. An outstanding tracking performance and robustness against lumped perturbations are achieved.

2 SMC design

2.1 System description

Consider a general dynamic system modelled using the differential equation, $\dot{\boldsymbol{x}} = (\boldsymbol{A} + \Delta\boldsymbol{A}(t,\boldsymbol{x}))\boldsymbol{x} + \boldsymbol{B}\boldsymbol{u} + \boldsymbol{w}(t,\boldsymbol{x})$, where $\boldsymbol{x} \in R^n$ is the state, $\boldsymbol{u} \in R^q$ is the control, $\boldsymbol{w}(t,\boldsymbol{x}) \in R^n$ is the disturbance, $\boldsymbol{A} \in R^{n\times n}$ is the system matrix, and the input matrix $\boldsymbol{B} \in R^{n\times q}$ is full ranked. The term $\Delta\boldsymbol{A}(t,\boldsymbol{x})$ represents the uncertain part of the system matrix. Let the term $\boldsymbol{v}(t,\boldsymbol{x})$ symbolise the lumped perturbations, i.e. $\boldsymbol{v}(t,\boldsymbol{x}) = \Delta\boldsymbol{A}(t,\boldsymbol{x})\boldsymbol{x} + \boldsymbol{w}(t,\boldsymbol{x})$. The new representation of the considered system becomes:

$$\dot{\boldsymbol{x}} = \boldsymbol{A}\boldsymbol{x} + \boldsymbol{B}\boldsymbol{u} + \boldsymbol{v}(t,\boldsymbol{x}) \tag{1}$$

In general, the SMC design is divided into two steps. The first step is to define the sliding functions such that the SMC system behaves like a prescribed linear system. The second step is to determine a control law such that the system will approach and proceed on the sliding hypersurface intersection.

The objective here is to place all of the closed-loop poles (n poles), instead of part of them ($n-q$ poles), and to eliminate the output errors.

2.2 Sliding function definition

Let $\boldsymbol{z} = [z_1, z_2, \ldots, z_q]^T = \boldsymbol{C}\boldsymbol{x}$ be the concerned outputs where $\boldsymbol{C} = [\boldsymbol{c}_1, \boldsymbol{c}_2, \ldots, \boldsymbol{c}_q]^T$. Define the output error as $\boldsymbol{e} = \boldsymbol{z} - \boldsymbol{z}_d$. The reference output $z_d = [z_{1d}, z_{2d}, \ldots, z_{qd}]^T$ is not restricted and, for example, can be generated from a reference model. For the sake of simplicity in this paper, we let z_d stand for the desired trajectory. The sliding function $\boldsymbol{\sigma}$ is defined as

IEE Proceedings online no. 20030593

doi: 10.1049/-i-cta:20030593

Paper first received 18th July 2002 and in revised form 25th April 2003

Y.J. Huang and T.C. Kuo are with the Department of Electrical Engineering, Yuan Ze University, 135 Far-East Rd., Chungli, Taiwan

H.K. Way is with the Department of Communication Engineering, National Chiao Tung University, 1001 University Rd., Hsinchu, Taiwan

$$\boldsymbol{\sigma} = \left[\sigma_1, \sigma_2, \ldots, \sigma_q\right]^{\mathrm{T}} = -\boldsymbol{G}\boldsymbol{x} + \boldsymbol{H}\int_0^t \boldsymbol{e}\,\mathrm{d}\tau \tag{2}$$

where the matrix $\boldsymbol{G} \in R^{q\times n}$ is selected such that $\boldsymbol{GB}$ is nonsingular. The weighting matrix $\boldsymbol{H} \in R^{q\times q}$ is selected to be full ranked.

Assumption 1: The pair $(\boldsymbol{A}, \boldsymbol{B})$ is completely controllable.

Assumption 2: Denote $\boldsymbol{G}_i$ as the ith row of the matrix $\boldsymbol{G}$ in (2). Let $\boldsymbol{\Gamma} = \mathrm{diag}\{\gamma_1, \gamma_2, \ldots, \gamma_q\}$, where $\gamma_i > 0$, $i = 1, \ldots, q$. For the lumped perturbations $\boldsymbol{v}(t,\boldsymbol{x}) = [\boldsymbol{v}_1(t,\boldsymbol{x}), \boldsymbol{v}_2(t,\boldsymbol{x}),\ldots,\boldsymbol{v}_n(t,\boldsymbol{x})]^T$, the following condition holds:

$$\|\boldsymbol{G}_i\boldsymbol{v}(t,\boldsymbol{x})\| \leqslant \gamma_i\|\boldsymbol{x}\|, \quad i = 1, \ldots, q \tag{3}$$

Theorem 1: Consider the system in (1) and the sliding function defined in (2). Let $\boldsymbol{G}$ be selected as:

$$\boldsymbol{G} = \boldsymbol{HCA}_{\mathrm{d}}^{-1} \tag{4}$$

where the matrix $\boldsymbol{A}_{\mathrm{d}} \in R^{n\times n}$ is the desired nonsingular closed-loop system matrix. Then, in the sliding mode, the closed-loop poles are exactly the eigenvalues of the desired system matrix $\boldsymbol{A}_{\mathrm{d}}$.

Proof: Suppose the sliding mode is attained within finite time. In the sliding mode, the linear equivalent control is generated by setting $\dot{\boldsymbol{\sigma}}$ to zero. This yields:

$$\boldsymbol{u}_{\mathrm{eq}} = -(\boldsymbol{GB})^{-1}\big(\boldsymbol{GAx} - \boldsymbol{He} + \boldsymbol{Gv}(t,\boldsymbol{x})\big) \tag{5}$$

The closed-loop state equation is then given by substituting (5) into (1):

$$\dot{\boldsymbol{x}} = \boldsymbol{A}_{\mathrm{eq}}\boldsymbol{x} + \boldsymbol{B}_{\mathrm{eq}}\boldsymbol{z}_{\mathrm{d}} \tag{6}$$

where

$$\boldsymbol{A}_{\mathrm{eq}} = \boldsymbol{A} - \boldsymbol{B}(\boldsymbol{GB})^{-1}(\boldsymbol{GA} - \boldsymbol{HC}) \tag{7}$$

$$\boldsymbol{B}_{\mathrm{eq}} = -\boldsymbol{B}(\boldsymbol{GB})^{-1}\boldsymbol{H} \tag{8}$$

Recall that the pair $(\boldsymbol{A}, \boldsymbol{B})$ is completely controllable for system (1). There always exists a non-zero matrix $\boldsymbol{K}$ such that the matrix:

$$\boldsymbol{A}_{\mathrm{d}} = \boldsymbol{A} + \boldsymbol{BK} \tag{9}$$

has arbitrarily assigned eigenvalues. For simplicity, the attention is subject to time-invariant systems, and the emphasis is that matrix $\boldsymbol{A}_{\mathrm{d}}$ can be arbitrarily assigned. For instance, one choice for $\boldsymbol{A}_{\mathrm{d}}$ might be the controllable canonical form:

$$\boldsymbol{A}_{\mathrm{d}} = \begin{bmatrix} 0 & 1 & 0 & \ldots & 0 \\ 0 & 0 & 1 & \ldots & 0 \\ \vdots & \vdots & \vdots & & \vdots \\ 0 & 0 & 0 & \ldots & 1 \\ -a_0 & -a_2 & -a_3 & \ldots & -a_{n-1} \end{bmatrix} \tag{10}$$

where $s^n + a_{n-1}s^{n-1} + \ldots + a_1 s + a_0 = 0$ is the desired closed-loop characteristic equation.

The weighting factor matrix $\boldsymbol{H}$ can be chosen in the simple form:

$$\boldsymbol{H} = \mathrm{diag}\{h_1, h_2, \ldots, h_q\} \tag{11}$$

where h_i, $i = 1, \ldots, q$, are the weighting factors for each output z_i respectively, and $h_i > 0$. Of course, the simplest form of $\boldsymbol{H}$ would be the identity matrix $\boldsymbol{I}_{q\times q}$, i.e. $h_i = 1$.

Since $\boldsymbol{A}_{\mathrm{d}}$ is nonsingular and $\boldsymbol{G} = \boldsymbol{HCA}_{\mathrm{d}}^{-1}$, the last term in (7) can be arranged to be $\boldsymbol{GA} - \boldsymbol{HC} = \boldsymbol{G}(\boldsymbol{A} - \boldsymbol{A}_{\mathrm{d}})$. Applying (9) yields:

$$\boldsymbol{A}_{\mathrm{eq}} = \boldsymbol{A} + \boldsymbol{B}(\boldsymbol{GB})^{-1}\boldsymbol{GBK} = \boldsymbol{A}_{\mathrm{d}} \tag{12}$$

Therefore, the linear equivalent system in the sliding mode is proven to have the desired closed-loop system matrix and hence the desired closed-loop poles.

2.3 Formulation of the control law

To meet the sliding condition:

$$\sigma_i\dot{\sigma}_i < 0 \tag{13}$$

let the control law be formulated as:

$$\boldsymbol{u} = \boldsymbol{\Lambda}\boldsymbol{x} + \boldsymbol{\Psi}\boldsymbol{e} + \boldsymbol{\Phi}\,\mathrm{sgn}\,(\boldsymbol{\sigma}) \tag{14}$$

where

$$\boldsymbol{\Lambda} = -(\boldsymbol{GB})^{-1}\boldsymbol{GA} \tag{15}$$

$$\boldsymbol{\Psi} = (\boldsymbol{GB})^{-1}\boldsymbol{H} \tag{16}$$

$$\boldsymbol{\Phi} = (\boldsymbol{GB})^{-1}\boldsymbol{\Gamma}\|\boldsymbol{x}\| \tag{17}$$

By taking the time derivative of both sides of (2) and applying (14)–(17), we obtain:

$$\dot{\boldsymbol{\sigma}} = -\boldsymbol{\Gamma}\|\boldsymbol{x}\|\mathrm{sgn}(\boldsymbol{\sigma}) - \boldsymbol{Gv}(t,\boldsymbol{x}) \tag{18}$$

For $i = 1, \ldots, q$:

$$\begin{aligned}\dot{\sigma}_i &= -\gamma_i\|\boldsymbol{x}\|\mathrm{sgn}(\sigma_i) - \boldsymbol{G}_i\boldsymbol{v}(t,\boldsymbol{x}) \\ &\leqslant -(\gamma_i\|\boldsymbol{x}\| - \|\boldsymbol{G}_i\boldsymbol{v}(t,\boldsymbol{x})\|\mathrm{sgn}(\sigma_i))\mathrm{sgn}(\sigma_i)\end{aligned} \tag{19}$$

Because the sum of the terms in the above brackets is larger than zero, the sliding condition (13) is therefore verified. The control law given by (14) guarantees that the sliding mode will be reached and sustained.

In summary, with the sliding function definition (2) and the control law (14), the sliding condition (13) will be satisfied. The larger γ_i is, the sooner the sliding mode is reached. The resulting control system has the following advantages:

(i) All of the closed-loop poles can be assigned.
(ii) The output errors effectively converge to zero.
(iii) The closed-loop system performance is robust.

3 VTOL aircraft control

3.1 Plant description

VTOL aircraft are complex, highly nonlinear systems whose aerodynamic parameters vary considerably during flight. Usually, the system dynamics can be linearised, and effective control methods can then be developed according to a linearised model.

Consider the typical load and flight conditions for a VTOL aircraft at the nominal airspeed of 135 knots [8, 9]. The linearised dynamics of this VTOL aircraft in the vertical plane can be described using:

$$\begin{aligned}\dot{\boldsymbol{x}} = &\begin{bmatrix} -0.0336 & 0.0271 & 0.0188 & -0.4555 \\ 0.0482 & -1.0100 & 0.0024 & -4.0208 \\ 0.1002 & 0.2855 & -0.7070 & 1.3229 \\ 0 & 0 & 1 & 0 \end{bmatrix}\boldsymbol{x} \\ &+ \begin{bmatrix} 0.4422 & 0.1761 \\ 3.0447 & -7.5922 \\ -5.5200 & 4.9900 \\ 0 & 0 \end{bmatrix}\boldsymbol{u} + \boldsymbol{v}(t,\boldsymbol{x})\end{aligned} \tag{20}$$

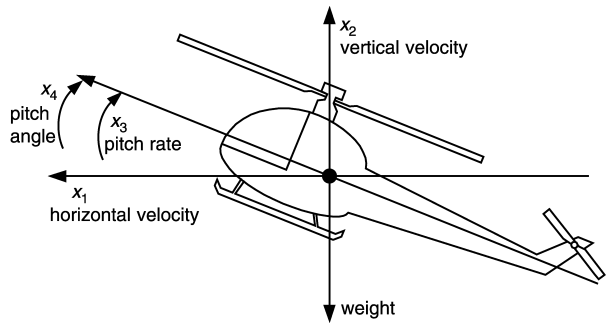

Fig. 1 *A typical sketch of a VTOL aircraft in a vertical plane*

The state vector $\boldsymbol{x} \in R^{4\times1}$ has the following components: x_1, horizontal velocity (knots); x_2, vertical velocity (knots); x_3, pitch rate (degrees per second); and x_4, pitch angle (degrees). Fig. 1 shows the typical coordinate system for a VTOL aircraft in the vertical plane. The control input $\boldsymbol{u} \in R^{2\times1}$ consists of the collective pitch control u_1, which alters the pitch angle (angle of attack with respect to the air) of the main rotor blades collectively to provide vertical movement, and the longitudinal cyclic pitch control u_2, which tilts the main rotor disc by varying the pitch of the main rotor blades individually to provide horizontal movement. However, u_1 and u_2 have some cross-effect on the vertical and horizontal velocities, respectively. The last term in (20) denotes the lumped perturbations, $\boldsymbol{v}(t,\boldsymbol{x}) = \Delta\boldsymbol{A}\boldsymbol{x}$ + wind gust. With airspeed ranging from 60 to 170 knots, significant changes occur in the elements $\boldsymbol{A}_{32}$ and $\boldsymbol{A}_{34}$, where $\boldsymbol{A}_{ij}$ denotes the ith row and jth column element of the matrix $\boldsymbol{A}$, assuming that $|\Delta\boldsymbol{A}_{32}| \leqslant 0.2192$ and $|\Delta\boldsymbol{A}_{34}| \leqslant 1.2031$.

The goal here is to develop a high performance VTOL aircraft control system using the sliding mode technique. The controller design should accomplish some practical objectives, such as: (i) enabling the VTOL aircraft to go from one initial state to the desired state rapidly; and (ii) minimising the sensitivity of the controlled variables when the VTOL aircraft is subject to parameter variations and disturbances.

3.2 SMC design

Using the optimal control approach [8], we can obtain the desired closed-loop system matrix:

$$\boldsymbol{A}_{\mathrm{d}} = \boldsymbol{A} + \boldsymbol{B}\begin{bmatrix} -0.8143 & -1.2207 & 0.2660 & 0.8260 \\ -0.2582 & 1.1780 & 0.0623 & -0.2120 \end{bmatrix} = \begin{bmatrix} -0.4422 & -0.3052 & 0.1474 & -0.1276 \\ -0.8779 & -14.2805 & 0.4723 & 0.5166 \\ 3.4358 & 12.3956 & -1.8956 & -4.0914 \\ 0 & 0 & 1 & 0 \end{bmatrix} \quad (21)$$

where the eigenvalues of $\boldsymbol{A}_{\mathrm{d}}$ are -0.6, -14.03 and $-0.67 \pm j1.76$.

Next, let $\boldsymbol{H} = \boldsymbol{I}_{2\times2}$. The sliding function is chosen with reference to (2), i.e.:

$$\boldsymbol{\sigma} = \begin{bmatrix} 1.9222 & -0.0991 & -0.0595 & -0.3606 \\ -0.0563 & 0.0778 & 0.0035 & -0.0115 \end{bmatrix}\boldsymbol{x} + \begin{bmatrix} \int_0^t (z_1 - z_{1\mathrm{d}})\mathrm{d}\tau \\ \int_0^t (z_2 - z_{2\mathrm{d}})\mathrm{d}\tau \end{bmatrix} \quad (22)$$

where z_1 and z_2 are the horizontal and vertical velocities, respectively, $z_{1\mathrm{d}}$ and $z_{2\mathrm{d}}$ are the horizontal and vertical velocity commands, respectively.

With the control law (14), the control input is determined to be:

$$\boldsymbol{u} = \begin{bmatrix} 0.0638 & -0.0241 & 0.2660 & 0.8260 \\ 0.0316 & -0.1436 & 0.0623 & -0.2120 \end{bmatrix}\boldsymbol{x} + \begin{bmatrix} 0.8781 & 1.1966 \\ 0.2898 & -1.3216 \end{bmatrix}\begin{bmatrix} z_1 - z_{1\mathrm{d}} \\ z_2 - z_{2\mathrm{d}} \end{bmatrix} + \begin{bmatrix} 0.8781 & 1.1966 \\ 0.2898 & -1.3216 \end{bmatrix}\begin{bmatrix} 0.4\|\boldsymbol{x}\|\mathrm{sat}\frac{\sigma_1}{0.05} \\ 0.3\|\boldsymbol{x}\|\mathrm{sat}\frac{\sigma_2}{0.05} \end{bmatrix} \quad (23)$$

In (23), the sliding layer technique [10] is utilised to further eliminate input chattering. The $\mathrm{sgn}(\boldsymbol{\sigma})$ function in (14) is replaced by the function $\mathrm{sat}(\boldsymbol{\sigma}/\delta)$, where $\delta > 0$ and for $\boldsymbol{\sigma} = [\sigma_1, \sigma_2, \ldots, \sigma_q]^{\mathrm{T}}$:

$$\mathrm{sat}\frac{\sigma_i}{\delta} = \begin{cases} \mathrm{sign}(\sigma_i), & |\sigma_i| > \delta \\ \frac{\sigma_i}{\delta}, & |\sigma_i| \leqslant \delta \end{cases} \quad i = 1, \ldots, q \quad (24)$$

The VTOL aircraft is assumed to be in forward flight and level attitude. The control sampling rate is set at 200 Hz. To compare the tracking and regulation capabilities, the following two cases are investigated:

Case 1: Vertical velocity command $z_{2\mathrm{d}} = 0.9(1 - e^{-2t})$ (normalised), while $z_{1\mathrm{d}} = 0$.

Case 2: Horizontal velocity command $z_{1\mathrm{d}} = 0.9(1 - e^{-2t})$ (normalised), while $z_{2\mathrm{d}} = 0$.

For both cases, nominal conditions with and without lumped perturbations are considered. A wind gust is supposed to occur at $t = 10\,s$, causing the VTOL aircraft to have a downward vertical constant acceleration of -1 (normalised).

3.3 Simulation result

3.3.1 Horizontal velocity and vertical velocity: Figs. 2–5 show the tracking performance of the vertical and horizontal velocities, respectively, of the proposed SMC. As can be seen, the tracking is fast and accurate. When the vertical motion proceeds, the horizontal direction maintains steady, and *vice versa*. The tracking errors converge to zero for the nominal systems. The effect of the parameter uncertainties is eliminated. When external disturbances occur, the SMC has the ability to drive the aircraft back to the desired trajectory rapidly, i.e. the flight

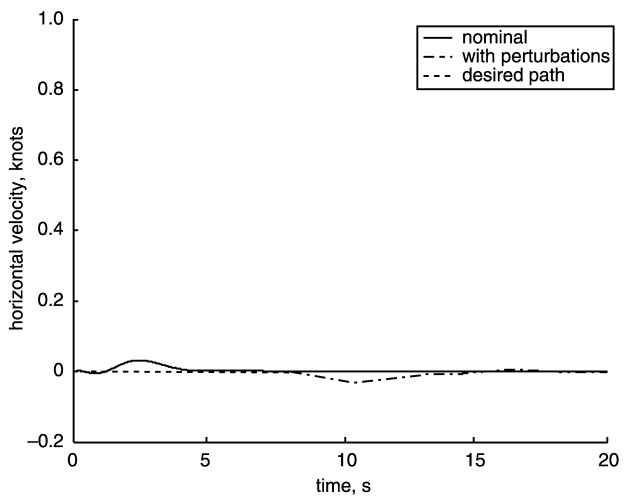

Fig. 2 *Horizontal velocities in case 1*

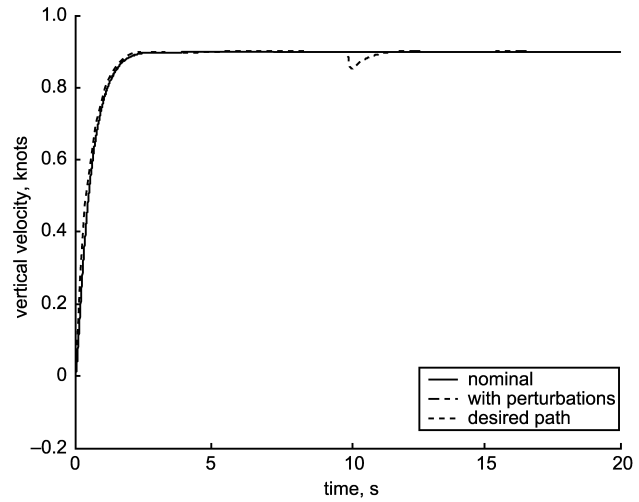

Fig. 3 *Vertical velocities in case 1*

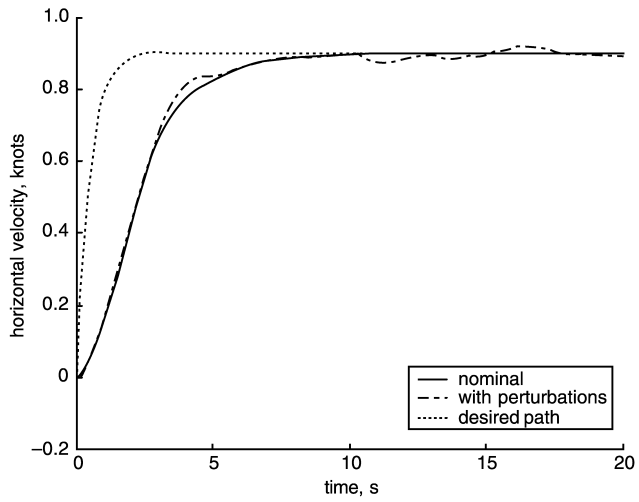

Fig. 4 *Horizontal velocities in case 2*

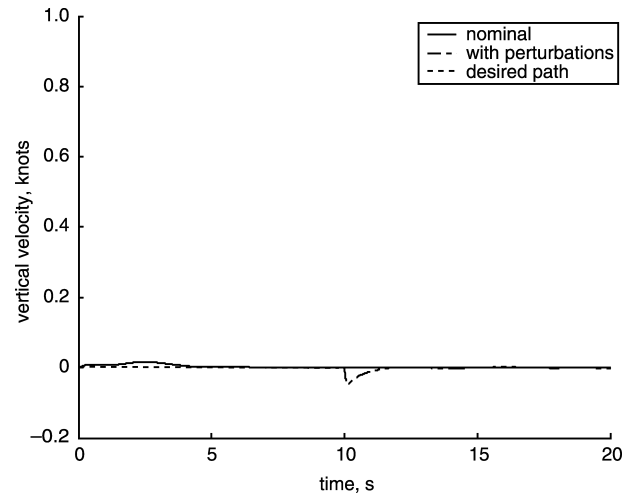

Fig. 5 *Vertical velocities in case 2*

will not be out of control against negative biased velocity disturbances.

3.3.2 Pitch rate and pitch angle: Because the system dynamics have a pair of complex closed-loop poles, the inherent transient state is observed in Figs. 6–9. The fast tracking response is achieved at the expense of oscillatory

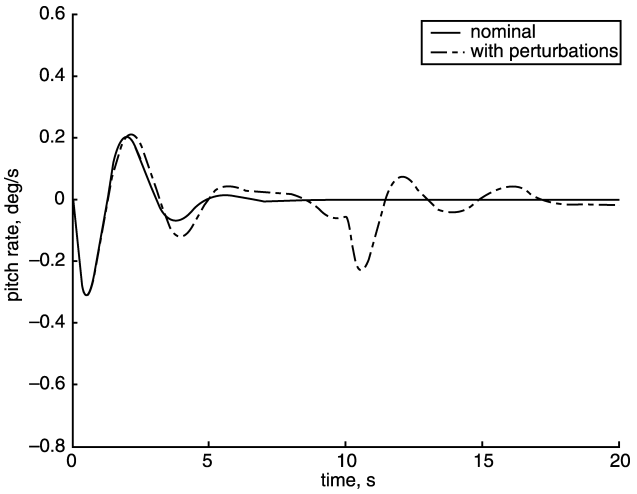

Fig. 6 *Pitch rates in case 1*

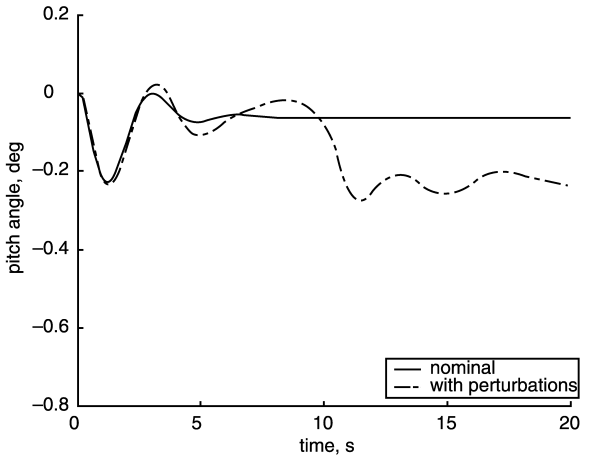

Fig. 7 *Pitch angles in case 1*

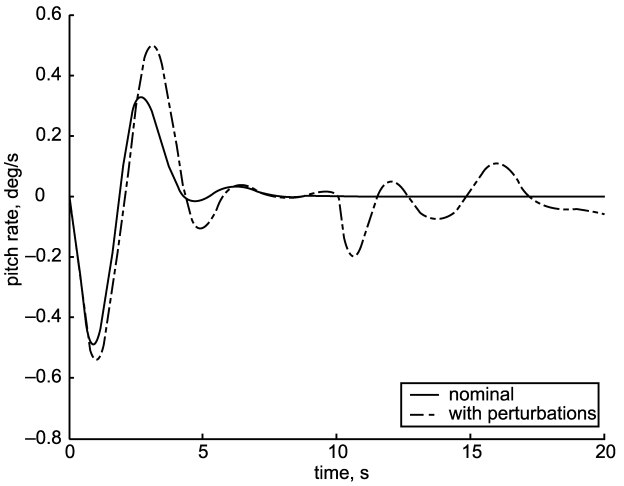

Fig. 8 *Pitch rates in case 2*

behaviour in the pitch angle and pitch rate. Yet the amplitudes are very small and acceptable in operation. In the presence of biased external disturbance, the aircraft exhibits small negative pitch angles to maintain the robustness.

3.3.3 Collective pitch and longitudinal cyclic pitch: As shown in Figs. 10–13, the control inputs tend to converge and the tracking errors converge in the first 10 s. The wind gust forces the control inputs to react abruptly.

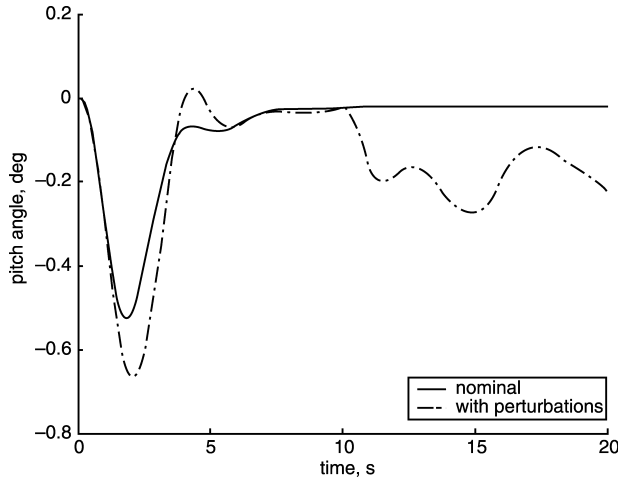

Fig. 9 *Pitch angles in case 2*

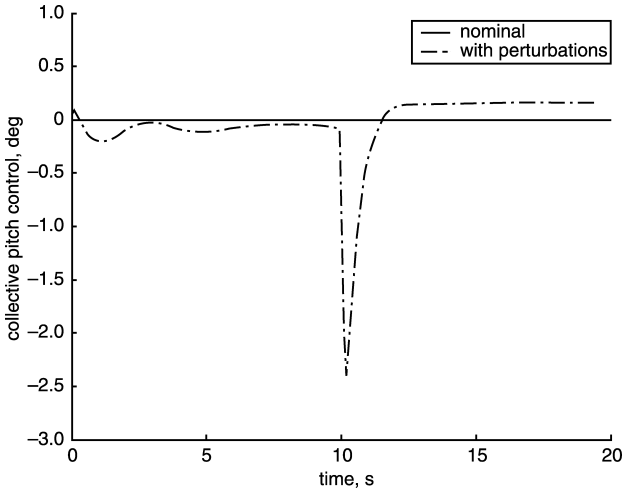

Fig. 10 *Collective pitch controls in case 1*

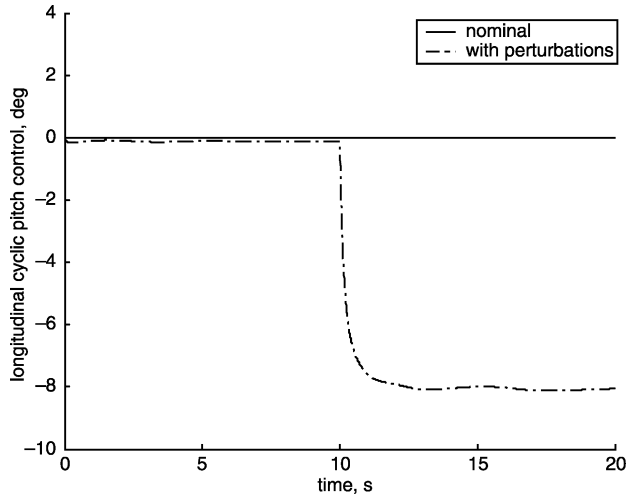

Fig. 11 *Longitudinal cyclic pitch controls in case 1*

The collective pitch reflects to a maximum, and then converges to a small positive position. Conversely, the longitudinal cyclic pitch reacts at about 8° negative deviation to maintain robust tracking purpose. The boundary layer technique is seen to be able to further eliminate input chattering.

Note that the closed-loop poles in the sliding mode can be freely assigned. The system response can be adjusted to be slower or faster so that the magnitudes of the collective pitch control and the longitudinal cyclic pitch control can become smaller or larger.

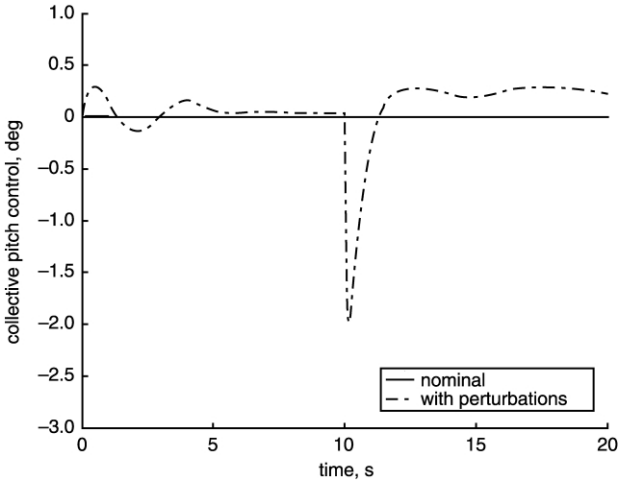

Fig. 12 *Collective pitch controls in case 2*

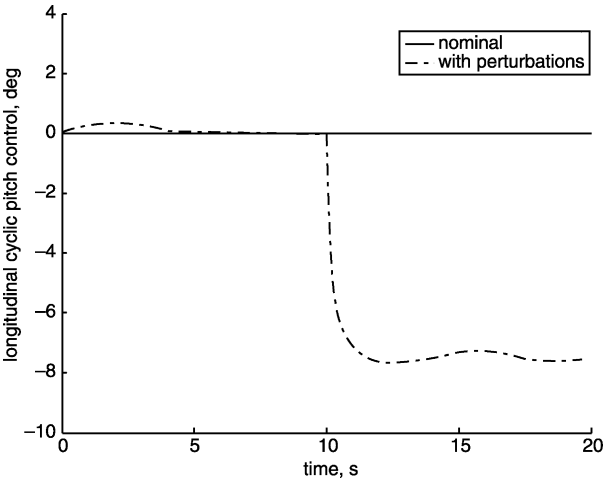

Fig. 13 *Longitudinal cyclic pitch controls in case 2*

4 Conclusions

A systematic SMC method has been presented. This design performs a full dimensional pole assignment in the sliding mode. All of the closed-loop poles can be assigned, not just those of the reduced systems. The sliding function involves the integral sliding mode. The control system is asymptotically stable and the output errors are eliminated. The application of the method to a VTOL aircraft control system has been successfully performed. The plant parameters vary with different operating conditions, and disturbances take place due to environmental changes. Due to the simple numerical computations, involved in the method the SMC response can be made faster than those of most other modern control methods. A remarkable tracking capability as well as system robustness was demonstrated.

5 Acknowledgments

The authors would like to thank the National Science Council, Taiwan, for supporting this work under grant NSC87-2623-D155-002.

6 References

1 Utkin, V.I.: 'Variable structure systems with sliding modes', *IEEE Trans. Autom. Cont.*, 1977, **22**, (2), pp. 212–222
2 Hung, J.Y., Gao, W., and Hung, J.C.: 'Variable structure control: a survey', *IEEE Trans. Ind. Electron.*, 1993, **40**, (1), pp. 2–22
3 Utkin, V.I., and Young, K.-K.D.: 'Methods for constructing discontinuity planes in multidimensional variable structure systems', *Autom. Remote Control*, 1979, **39**, (10), pp. 1466–1470
4 Su, W.C., Drakunov, S.V., and Özgüner, Ü.: 'Constructing discontinuity surfaces for variable structure systems: a Lyapunov approach', *Automatica*, 1996, **32**, (6), pp. 925–928
5 El-Ghezawi, O.M.E., Zinober, A.S.I., and Billings, S.A.: 'Analysis and design of variable structure systems using a geometric approach', *Int. J. Control*, 1983, **38**, (3), pp. 657–671
6 Dorling, C.M., and Zinober, A.S.I.: 'Two approaches to hyperplane design in multivariable variable structure systems', *Int. J. Control*, 1986, **44**, (1), pp. 65–82
7 Huang, Y.J., and Way, H.K.: 'Design of sliding surfaces in variable structure control via direct pole assignment scheme', *Int. J. Syst. Sci.*, 2001, **32**, (8), pp. 963–969
8 Singh, S.N., and Coelho, A.A.R.: 'Nonlinear control of mismatched uncertain linear systems and application to control of aircraft', *Trans. ASME, J. Dyn. Syst. Meas. Control*, 1984, **106**, pp. 203–210
9 Schmitendorf, W.E.: 'Design methodology for robust stabilizing controllers', *J. Guid.*, 1987, **10**, (3), pp. 250–254
10 Slotine, J.J., and Sastry, S.S.: 'Tracking control of non-linear system using sliding surfaces with application to robot manipulators', *Int. J. Control*, 1983, **38**, (2), pp. 465–492